INTERNATIONAL JOURNAL OF ENERGY STUDIES

e-ISSN: 2717-7513 (ONLINE); homepage: https://dergipark.org.tr/en/pub/ijes

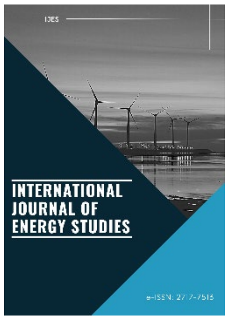

Research Article

Int J Energy Studies 2025; 10(2): 332-366

DOI: 10.58559/ijes.1639324

Received : 13 Feb 2025
Revised : 9 Apr 2025
Accepted : 14 Apr 2025

Thermodynamic insights and comparative evaluation of R22, R410A, R32, R290, and R1234ze(E) in air source heat pump systems: A theoretical study

Kutbay Sezen[a*]

[a]*Department of Air Conditioning and Refrigeration Technology, ALTSO Vocational School, Alanya Alaaddin Keykubat University, Antalya, Türkiye, ORCID: 0000-0003-1018-5793*

*(*Corresponding Author: kutbay.sezen@alanya.edu.tr)*

Highlights

- R32 excels in cold conditions but its future is limited vs. new-gen refrigerants
- R1234ze(E) requires larger pipes to mitigate pressure losses
- Flammable R290 balances safety with lower operating pressures
- Phased-out R410A and R22 require higher mass flow rates and charges

You can cite this article as: Sezen K. Thermodynamic insights and comparative evaluation of R22, R410A, R32, R290, and R1234ze(E) in air source heat pump systems: a theoretical study. Int J Energy Studies 2025; 10(2): 332-366

ABSTRACT

Air source heat pumps (ASHPs), particularly split air conditioners, are widely favored for their energy efficiency, ease of application, and capacity to provide both seasonal heating and cooling. However, their performance and environmental impact are largely determined by the refrigerants they use. This study examines the performance and operating parameters of an ASHP retrofitted with five different refrigerants—R22, R410A, R32, R290, and R1234ze(E)—using a physics-based model. R22 and R410A were considered phased-out refrigerants due to their environmental impact, while R32, R290, and R1234ze(E) were evaluated as eco-friendly pure refrigerant alternatives. Refrigerants were analyzed at outdoor temperatures of 0°C, 7°C, and 15°C, with evaporator and condenser pressure drops included to improve model accuracy. R32 demonstrated superior coefficient of performance (COP) at lower outdoor temperatures, while R1234ze(E) outperformed other refrigerants at 15°C. R1234ze(E) exhibited the highest refrigerant flow rate, nearly twice that of R290 and R32, increasing charging costs. However, its low condensing pressure allows for more economical equipment. R290 showed the lowest pressures, facilitating safer sealing despite its high flammability. Pressure drop and pipe diameter requirements are critical in system design. R1234ze(E) requires larger pipes to mitigate pressure losses, increasing system costs and refrigerant charge. R32, with minimal pressure loss, allows smaller pipes, making it cost-effective. R290, though needing slightly larger pipes than R32, operates at lower condenser and evaporator pressures, improving safety and reducing sealing challenges. This feature, combined with its low GWP, makes R290 a promising next-generation refrigerant, though its high flammability remains a concern. R32 consistently achieves the lowest condensing temperatures at lower outdoor conditions. These findings provide insights into the trade-offs between environmental benefits, performance, and operational considerations of various refrigerants.

Keywords: Air source heat pump, Refrigerant performance analysis, Low GWP refrigerants, Thermodynamic model

1. INTRODUCTION

In the industrializing and urbanizing world, the heating needs of living and working environments are increasing in parallel with the overall rising energy demand. Air source heat pumps (ASHPs) are widely preferred by users due to their energy-efficient features, ease of application, and ability to provide both seasonal heating and cooling. Among these systems, split air conditioners, which offer room-based usage, are particularly popular and widely available in the consumer market.

Despite their advantages, air conditioners rely on refrigerants that play a critical role in their performance and environmental impact. The use of refrigerants in air conditioning and heat pump systems has been significantly shaped by international environmental agreements, beginning with the Montreal Protocol in 1987. This landmark treaty was established to address the alarming depletion of the ozone layer caused by chlorofluorocarbons (CFCs) and hydrochlorofluorocarbons (HCFCs). Among these, R22, an HCFC, was widely used in air conditioning systems due to its excellent thermodynamic properties and reliability. However, its high ozone depletion potential (ODP) led to its gradual phase-out under the Montreal Protocol, with developed countries ceasing production by 2020 and developing countries following suit by 2030 [1]. This phase-out marked the beginning of a global shift toward hydrofluorocarbons (HFCs), such as R410A, which have zero ODP but still pose environmental challenges due to their high global warming potential (GWP). R410A, a mixture of 50% R32 and 50% R125, has a high GWP primarily attributed to the R125 component [2]. While R410A addressed ozone layer concerns, its significant GWP has prompted further regulatory action under the Kigali Amendment (2016), driving the search for eco-friendlier refrigerants [3].

The Kigali Amendment to the Montreal Protocol, adopted in 2016, represents a critical step in addressing the climate impact of HFCs. It mandates a phasedown of HFCs, aiming to reduce their production and consumption by 80–85% by 2047, which is expected to prevent up to 0.5°C of global warming by the end of the century [3]. Central to this effort is the use of the CO2 equivalent (CO2e) concept, which quantifies the climate impact of greenhouse gases relative to carbon dioxide. For example, R410A has a GWP of 2,088, meaning it has 2,088 times the warming potential of CO2 over a 100-year period [2]. This metric guides the transition to low-GWP alternatives, such as hydrofluoroolefins (HFOs) and natural refrigerants like R290 (propane) and R1234ze(E). These next-generation refrigerants offer a balance between environmental sustainability and thermodynamic performance, aligning with global efforts to combat both ozone depletion and climate change. The transition from HCFCs to HFCs and now to low-GWP alternatives reflects the ongoing evolution of refrigerant technology in response to stringent environmental regulations [3, 4].

As the search for low-GWP alternatives continues, newer refrigerants like R32, R290, and R1234ze(E) have emerged. R32, another hydrofluorocarbon (HFC), offers a 32% lower GWP compared to R410A, along with higher energy efficiency and low cost [5]. However, its mild flammability requires careful handling and system design considerations. R290 (propane), a hydrocarbon (HC) refrigerant, and R1234ze(E), a hydrofluoroolefin (HFO), represent the latest generation of refrigerants, boasting ultra-low GWPs and enhanced environmental sustainability [6, 7]. Despite their advantages, R290's high flammability and R1234ze(E)'s high-cost present notable challenges [8, 9].

Table 1 summarizes the key properties of the five refrigerants, including ozone depletion potential (ODP), global warming potential (GWP), flammability, and cost. The data are synthesized from key review studies in the literature. The cost categories (low, medium, high) are based on the relative market prices and production costs of the refrigerants. Low cost refers to refrigerants that are widely available, easy to produce, and have lower market prices (e.g., R290). Medium cost indicates refrigerants with moderate production costs and market prices, often due to established manufacturing processes and supply chains (e.g., R22, R410A, R32). High cost refers to refrigerants that are newer to the market, require advanced production techniques, or have limited availability, resulting in higher prices (e.g., R1234ze(E)). This classification provides a general overview of the economic considerations associated with each refrigerant.

Table 1. Properties of refrigerants [9-12]

Refrigerant	ODP	GWP	Cost	Flammability	Atmosp. Life (years)	Molecular Weight (g/mol)	Critical Temp. (°C)	Critical Pressure (kPa)	Latent Heat of Vaporization (kJ/kg)
R22	0.055	1810	Medium	None (A1)	12	86.47	96.2	4990	233.9
R410A	0	2088	Medium	None (A1)	16.5	72.58	72.1	4920	256.7
R32	0	677	Medium	Low (A2L)	5.2	52.02	78.1	5782	389.1
R290	0	3.0	Low	High (A3)	0.04	44.10	96.7	4248	426
R1234ze(E)	0	6.0	High	Low (A2L)	0.03	114.04	109.4	3636	161.2

The refrigerants in this study were selected based on their thermophysical properties, environmental impact, and suitability for split air conditioning systems. While R22, R410A, and

R32 are commonly used, R290 (propane) and R1234ze(E) are promising next-generation alternatives. R290 has a very low GWP (3.0), zero ODP, and high latent heat of vaporization (426.0 kJ/kg), making it efficient and environmentally friendly. R1234ze(E) offers a negligible GWP (6.0), zero ODP, and low flammability (A2L classification), ensuring safety and compliance with regulations like the Kigali Amendment. Both refrigerants have short atmospheric lifetimes (0.04 and 0.03 years, respectively), minimizing their environmental impact. However, their adoption requires careful consideration of safety standards and system design due to flammability and thermodynamic characteristics.

Several studies have examined the performance and system parameters of new refrigerants, providing insights into their applicability and challenges. Shaik and Babu [13] performed a theoretical thermodynamic analysis of R22 alternatives, finding that a blend of R134a/R1270/RE170 (55/37.5/7.5 by mass) achieved a 5.35% higher COP and significantly lower GWP compared to R22, highlighting its potential as a sustainable alternative. Martins et al. [14] assessed R22 replacements in single split air conditioners, identifying R444B as a better option at mild temperatures, offering a 15% higher COP and 55% lower TEWI compared to R22. Katircioğlu et al. [15] evaluated alternatives to R22, finding R438A as a suitable replacement with comparable performance metrics and enhanced environmental benefits.

In the context of R410A, Fajar et al. [16] studied the replacement of R410A with R290 in small vapor compression systems, demonstrating a 6.5% improvement in COP at optimal charge levels, though refrigerating capacity and compressor power consumption were reduced by 31.3% and 35.7%, respectively. Guilherme et al. [17] reviewed low-GWP alternatives to R410A, identifying HFO/HFC blends DR-55 and DR-5A as promising drop-in candidates with comparable cooling capacities and significantly reduced TEWI and LCCP values.

R32, another viable alternative, has been widely studied. Tian et al. [18] demonstrated that a refrigerant mixture of R32/R290 (68/32% by weight) reduced GWP by 78% compared to R410A while improving cooling capacity by 14%–23.7% and COP by 6.8% with reduced refrigerant charge requirements. Similarly, Mota-Babiloni et al. [5] highlighted R32's potential in residential air conditioners in Europe and the USA, emphasizing its improved energy efficiency and acceptable flammability compared to R410A.

Other studies have focused on R1234ze(E), a hydrofluoroolefin (HFO) refrigerant. Mota-Babiloni et al. [19] evaluated its performance in heat pumps, finding comparable COP and up to 28% lower equivalent carbon emissions compared to R134a. Zhang and Li [20] reviewed recent research on HFOs, emphasizing R1234ze(E)'s environmental benefits and compatibility with HVAC systems. However, they noted the need for further investigation into its thermophysical properties and decomposition mechanisms. Salhi et al. [21] demonstrated that HFO refrigerants like R1234yf, R1234ze(E), and R1233zd(E) in solar-assisted air conditioning systems can improve efficiency by up to 56% and significantly reduce electrical energy consumption.

Hydrocarbons such as R290 have also been extensively studied for their environmental and performance characteristics. Ibrahim et al. [22] reviewed hydrocarbon refrigerants, demonstrating R290's excellent COP and thermophysical properties but emphasizing challenges related to its high flammability. Choudhari and Sapali [23] compared R290 with R22, finding that while R290 exhibited slightly lower COP, it is a better long-term alternative due to its superior environmental properties. Singh et al. [24] analyzed 22 natural refrigerant pairs for a cascade refrigeration system and found that R717-R290 is the most thermodynamically efficient pair, while R600a-R290 is the least economical option. Koşan [25] investigated six alternatives to high-GWP R404A and concluded that R290 and R1270 offered the best performance as low-GWP options.

Innovative refrigerant blends and configurations have also been explored. Stegou-Sagia and Damanakis [26] investigated binary refrigerant mixtures such as R32/R134a, presenting COP data under various thermodynamic conditions. Tamene et al. [7] evaluated eco-friendly azeotropic mixtures like R1234yf+R290, which offered superior performance and lower GWP compared to R134a, particularly in ejector-expansion refrigeration cycles. Ravi and Adhimoulame [27] analyzed refrigerant blends involving R290 and R1234ze(E), showing that such combinations can outperform R1234ze(E) in efficiency and environmental impact.

The reviewed studies collectively demonstrate the growing potential of low-GWP refrigerants like R32, R290, R1234ze(E), and their blends as alternatives to traditional refrigerants. However, while blends have been proposed for optimizing performance and environmental characteristics, they often introduce practical challenges, such as service difficulties during gas leakage and the need for complete evacuation and refilling. These issues can increase operational complexity and costs, limiting their practicality in real-world applications.

In contrast to studies focusing on blended refrigerants, this study examines pure refrigerants, which offer greater ease of service and practical applicability. While several studies have assessed the performance of individual refrigerants and their blends, relatively few have directly compared the effects of past refrigerants (R22, R410A) and emerging pure refrigerant options (R32, R290, R1234ze(E)) on ASHP performance under varying operating conditions. This gap is particularly significant given the need for a comprehensive understanding of how these refrigerants perform in real-world scenarios. By focusing on pure refrigerants and employing a physics-based model, this study provides a novel and practical perspective on the transition to next-generation refrigerants.

This study addresses these gaps by providing a collective comparison of R22, R410A, R32, R290, and R1234ze(E) in a reference ASHP system under varying outdoor conditions (0 °C, 7 °C, and 15 °C). An inverter split air conditioner with a nominal heating capacity of 4.6 kW using R32 refrigerant was selected as the reference system. The physics-based model used in this study was developed and validated in two prior works by the authors. The first study [28] investigated the effects of outdoor temperature and relative humidity on ASHP performance, while the second study [29] examined the impact of evaporator and condenser airflow rates. In contrast, this study applies the model to a new research aim: investigating the effects of different refrigerants (R22, R410A, R32, R290, and R1234ze(E)) on ASHP performance and identifying design challenges. Using the physics-based model, the systems were analyzed to evaluate key performance metrics such as coefficient of performance (COP), refrigerant mass flow rates, and system pressures for different refrigerants. The results provide a comprehensive understanding of how these refrigerants perform under varying conditions, contributing to the development of more efficient and sustainable ASHP technologies.

2. METHODOLOGY

2.1. Physics-based Model

A split air conditioner, operating as an air source heat pump (ASHP), transfers heat from the outdoor air (the heat source) to the indoor environment via the refrigerant, with the addition of compressor power. This process involves heat exchange between the air and the refrigerant within the condenser and evaporator. To accurately model the ASHP using a physics-based approach, it is essential to analyze the heat transfer processes occurring in the evaporator and condenser heat exchangers alongside the thermodynamic cycle of the refrigerant.

The system was modeled by building upon the approach specified in the study by Sezen and Gungor [28], which examined the effects of outdoor air temperature and humidity on the performance of the ASHP system. This approach was later applied in Sezen's [29] subsequent study to investigate the impact of evaporator and condenser air flow rates on ASHP performance. In the present study, the same approach was adapted to model the ASHP system and analyze the effects of different refrigerant types.

2.1.1. Assumptions

The following assumptions were made to simplify the model and facilitate its solution:

- Pressure losses at intermediate pipelines were neglected.
- The isentropic efficiency and global efficiency of the compressor were assumed to remain constant.
- Expansion in the thermal expansion valve was considered isenthalpic.
- Superheat and subcooling values were set to 5°C.
- No heat loss to the surrounding environment was assumed at any point in the system.

2.1.2. System components and interactions

The components of the air source heat pump and their interactions with indoor and outdoor air are illustrated in Fig. 1. The properties of the refrigerant vary as state changes occur in each component. Similarly, the indoor and outdoor air undergo state changes due to heat transfer in the condenser and evaporator, respectively.

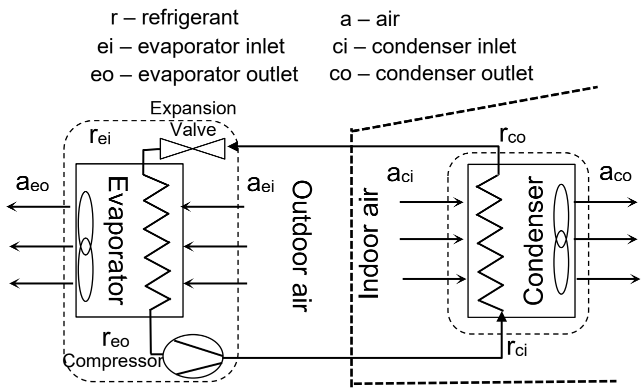

Figure 1. The components of the ASHP and their interactions with indoor and outdoor air

Modeling the system requires determining the changing properties of both the refrigerant and the air. To achieve this, the CoolProp program, which integrates seamlessly with MS Excel, was utilized. CoolProp calculates desired properties of various refrigerants using two known properties based on its embedded equations of state [30]. Likewise, it can determine any psychrometric property of air given two known input properties.

The modeling of the air source heat pump can be accomplished by defining the state changes of the refrigerant within each component and its interactions with the air, where applicable. Subsequently, the impact of using different refrigerants on this state change mechanism should be analyzed.

2.1.3. Heat exchanger modeling

The evaporator and condenser are modeled as finned counterflow heat exchangers, where the refrigerant exchanges heat with outdoor and indoor air, respectively.

2.1.3.1. Evaporator heat transfer

The heat transfer in the evaporator can be expressed using the total heat transfer coefficient, UA_e, and the logarithmic mean temperature difference of the evaporator, ΔT_{me}, as shown in Eq. (1):

$$\dot{Q}_e = UA_e \Delta T_{me} \tag{1}$$

The total heat transfer coefficient of the evaporator, UA_e, can be determined using the NTU value provided in the manufacturer's catalog, as expressed in Eq. (2).

$$UA_e = C_{e\_min} . NTU_e \tag{2}$$

Here, C_{e_min} is the heat capacity of the smaller value between the refrigerant and air pair. Since the heat capacity of the air, which experiences a temperature decrease compared to the evaporating refrigerant, is significantly lower, the heat capacity of the air should be used.

$$C_{e\_min} = \dot{m}_{ae} . c_{ae} \tag{3}$$

Here, $\dot{m}_{ae}$ represents the air flow rate through the evaporator, and c_{ae} is the average specific heat capacity of the air.

Since the heat transfer resistance is primarily on the air side, the NTU_e value can be assumed unchanged despite changes in refrigerant type. Therefore, it can also be assumed that the total heat transfer coefficient of the evaporator, UA_e, remains unchanged when using different refrigerants and fixed air flow rate.

In this case, as shown in Eq. (4), a direct proportionality can be defined between the evaporator heat load and the logarithmic mean temperature difference ΔT_{me} formed between the air and the refrigerant in the evaporator:

$$\frac{\dot{Q}_e|_{r2}}{\dot{Q}_e|_{r1}} = \frac{\Delta T_{me}|_{r2}}{\Delta T_{me}|_{r1}} \tag{4}$$

Here, the subscripts $r1$ and $r2$ represent the use of different refrigerants.

The logarithmic mean temperature difference ΔT_{me} in the evaporator is illustrated in Fig. 2.

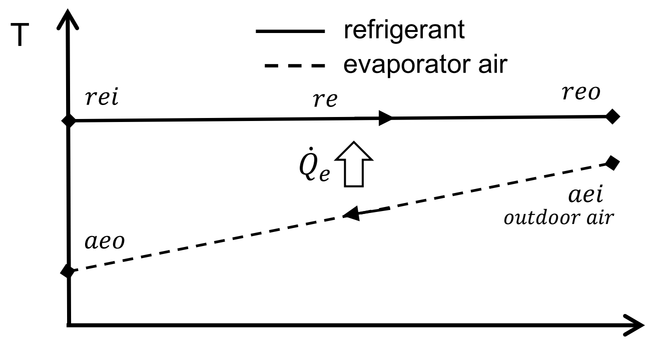

Figure 2. Heat exchange between refrigerant and air in the evaporator

The logarithmic mean temperature difference ΔT_{me} of the evaporator is defined in Eq. (5).

$$\Delta T_{me} = \frac{(T_{aei}-T_{re})-(T_{aeo}-T_{re})}{\ln\frac{(T_{aei}-T_{re})}{(T_{aeo}-T_{re})}} \tag{5}$$

Here, T_{aei} is the temperature of the outdoor air entering the evaporator, T_{aeo} is the temperature of the air exiting the evaporator, and T_{re} is the evaporation temperature of the refrigerant.

2.1.3.2. Condenser heat transfer

For the condenser, it is a more accurate approach to divide the heat transfer process into two regions, as shown in Figure 3, when defining the logarithmic mean temperature difference ΔT_{mc}.

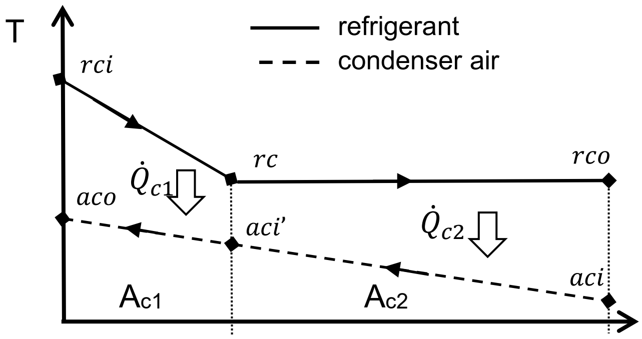

Figure 3. Heat exchange between refrigerant and air in the condenser

The condenser heat load can be defined as the sum of the heat transfer occurring in the two regions, as shown in Eqs. (6) and (7).

$$\dot{Q}_c = \dot{Q}_{c1} + \dot{Q}_{c2} \tag{6}$$

$$\dot{Q}_c = U_c A_{c1} \Delta T_{mc1} + U_c A_{c2} \Delta T_{mc2} \tag{7}$$

Here, A_{c1} and A_{c2} represent the areas of the first and second regions in the condenser where heat transfer occurs, respectively. ΔT_{mc1} and ΔT_{mc2} denote the logarithmic mean temperature differences in these regions and can be defined using Eqs. (8) and (9).

$$\Delta T_{mc1} = \frac{(T_{rci} - T_{aco}) - (T_{rc} - T_{aci'})}{\ln \frac{(T_{rci} - T_{aco})}{(T_{rc} - T_{aci'})}} \tag{8}$$

$$\Delta T_{mc2} = \frac{(T_{rc} - T_{aci}) - (T_{rc} - T_{aci'})}{\ln \frac{(T_{rc} - T_{aci})}{(T_{rc} - T_{aci'})}} \tag{9}$$

Here, T_{rc} is the condensation temperature of the refrigerant, and T_{rci} is the refrigerant temperature at the condenser inlet. T_{aci} is the condenser inlet air temperature, which can be taken as the indoor air temperature. $T_{aci'}$ is the intermediate air temperature reached during the second region due to refrigerant condensation. T_{aco} is the condenser outlet air temperature, which varies depending on the required heat load in an inverter air conditioner.

For a constant air flow rate in the condenser, as in the evaporator, it can be assumed that the total heat transfer coefficient, UA_c, remains unchanged when using different refrigerants.

The variation in the logarithmic temperature difference for the second region, which is responsible for the majority of the condenser heat load, can be expressed as shown in Eq. (10), depending on the use of different refrigerants.

$$\frac{\Delta T_{mc2}|_{r2}}{\Delta T_{mc2}|_{r1}} = \frac{\dot{Q}_{c2}\big|_{r2}}{\dot{Q}_{c2}\big|_{r1}} \cdot \frac{A_{c2}|_{r1}}{A_{c2}|_{r2}} \tag{10}$$

Eq. (10) can be expanded through the following steps:

$$\frac{\Delta T_{mc2}|_{n}}{\Delta T_{mc2}|_{0}} = \frac{\left.\frac{\dot{Q}_{c2}}{\dot{Q}_{c}}\right|_{n}}{\left.\frac{\dot{Q}_{c2}}{\dot{Q}_{c}}\right|_{0}} \cdot \frac{\left.\frac{A_{c2}}{A_{c}}\right|_{0}}{\left.\frac{A_{c2}}{A_{c}}\right|_{n}} \cdot \frac{\dot{Q}_{c}\big|_{n}}{\dot{Q}_{c}\big|_{0}} \cdot \frac{U_{c}|_{0}}{U_{c}|_{n}} \tag{11}$$

$$\frac{\Delta T_{mc2}|_{n}}{\Delta T_{mc2}|_{0}} = \frac{\left.\frac{\dot{Q}_{c2}}{\dot{Q}_{c}}\right|_{n}}{\left.\frac{\dot{Q}_{c2}}{\dot{Q}_{c}}\right|_{0}} \cdot \frac{\left.\frac{A_{c2}}{A_{c1}}/(1+\frac{A_{c2}}{A_{c1}})\right|_{0}}{\left.\frac{A_{c2}}{A_{c1}}/(1+\frac{A_{c2}}{A_{c1}})\right|_{n}} \cdot \frac{\dot{Q}_{c}\big|_{n}}{\dot{Q}_{c}\big|_{0}} \cdot \frac{U_{c}|_{0}}{U_{c}|_{n}} \tag{12}$$

$$\frac{A_{c2}}{A_{c1}} = \frac{\dot{Q}_{c2}}{\dot{Q}_{c1}} \cdot \frac{\Delta T_{mc1}}{\Delta T_{mc2}} \tag{13}$$

The heat loads of the condenser regions, $\dot{Q}_{c1}$ and $\dot{Q}_{c2}$, can be calculated based on the enthalpy change of the refrigerant using Eqs. (14) and (15).

$$\dot{Q}_{c1} = \dot{m}_r\left(h_{rci} - h_{rcg}\right) \tag{14}$$

$$\dot{Q}_{c2} = \dot{m}_r\left(h_{rcg} - h_{rco}\right) \tag{15}$$

Here, h_{rci} represents the refrigerant enthalpy at the condenser inlet, h_{rcg} is the enthalpy of the refrigerant at the onset of condensation, and h_{rco} is the refrigerant enthalpy at the condenser outlet.

2.1.4. Energy balance

The compressor's output power $\dot{W}_{Co}$ transferred to the refrigerant can be expressed using Eq. (16), based on the input power $\dot{W}_{Ci}$ drawn from the network and the compressor's global efficiency η_{cg}.

$$\dot{W}_{Co} = \dot{W}_{Ci} \cdot \eta_{cg} \tag{16}$$

The coefficient of performance (COP) of the ASHP is defined as the ratio of the heat provided to the power consumed, as shown in Eq. (17).

$$COP = \frac{Condenser\ heating\ load}{Total\ input\ power\ of\ comp.and\ fans} = \frac{\dot{Q}_c}{\dot{W}_{Ci}+\dot{W}_{fi}} \tag{17}$$

Using the energy balance of the refrigerant, the evaporator heat load ($\dot{Q}_e$) can be defined by Eq. (18).

$$\dot{Q}_c = \dot{Q}_e + \dot{W}_{Co} \tag{18}$$

The condenser inlet enthalpy can be determined using the compressor isentropic efficiency η_{cs}, as shown in Eq. (19).

$$h_{rci} = (h_{rcis} - h_{reo})/\eta_{cs} + h_{reo} \tag{19}$$

Here, h_{rcis} is the condenser inlet enthalpy that would be reached under isentropic compression, and it can be determined using the condenser pressure P_c and the evaporator outlet entropy s_{reo}.

The compressor output power and the heat loads of the condenser and evaporator can be expressed in terms of refrigerant flow rate and enthalpy changes using Eq. (20),
Eq. (21), and Eq. (22), respectively.

$$\dot{W}_{Co} = \dot{m}_r(h_{rci} - h_{reo}) \tag{20}$$

$$\dot{Q}_c = \dot{m}_r(h_{rci} - h_{rco}) \tag{21}$$

$$\dot{Q}_e = \dot{m}_r(h_{reo} - h_{rei}) \tag{22}$$

The heat loads of the condenser regions can be expressed in terms of the condenser air flow rate ($\dot{m}_{ac}$) and the air enthalpy change using Eqs. (23) and (24).

$$\dot{Q}_{c1} = \dot{m}_{ac}(h_{aco} - h_{aci\prime}) \tag{23}$$

$$\dot{Q}_{c2} = \dot{m}_{ac}(h_{aci\prime} - h_{aci}) \tag{24}$$

The evaporator heat load is defined in terms of the evaporator air flow rate ($\dot{m}_{ae}$) and the air enthalpy change, as shown in Eq. (25).

$$\dot{Q}_e = \dot{m}_{ae}(h_{aei} - h_{aeo}) \tag{25}$$

Assuming that the building's heat loss varies with the outdoor-to-indoor temperature difference, the variation in the condenser heat load requirement can be defined using Eq. (26).

$$\frac{\dot{Q}c|_n}{\dot{Q}c|_0} = \frac{(T_{ai}-T_{ao})|_n}{(T_{ai}-T_{ao})|_0} \tag{26}$$

2.1.5. Pressure drop calculations

The pressure drops in the two-phase sections of the evaporator ($\varDelta P_{tpe}$) and condenser ($\varDelta P_{tpc}$) finned tubes were calculated using the correlation by Choi et al.[31], as applied in Koopman et al. [32], which accounts for both friction ($\varDelta P_{fr}$) and acceleration ($\varDelta P_{acc}$) components:

$$\varDelta P_{tp} = \varDelta P_{fr} + \varDelta P_{acc} = \left(\frac{f_N L_{tp}(\nu_{out}-\nu_{in})}{D_h} + (\nu_{out} - \nu_{in})\right) G^2 \tag{27}$$

Where f_N is the two-phase friction factor, L_{tp} is the length of the two-phase section, ν represents the specific volume of the two-phase fluid at the inlet and outlet of the segment L, D_h is the hydraulic diameter, and G is the mass flux of the refrigerant, defined as the mass flow rate per unit of cross-sectional area.

The two-phase friction factor is defined as:

$$f_N = 0.00506\, {Re_{fo}}^{-0.0951}\, {K_f}^{0.1554} \tag{28}$$

where Re_{fo} is the liquid-only Reynolds number, given by:

$$Re_{fo} = \frac{GD_h}{\mu_f} \tag{29}$$

and K_f is the two-phase number, expressed as:

$$K_f = \frac{\Delta_x h_{fg}}{L\, g} \tag{30}$$

The evaporator can be assumed to be entirely in the two-phase region when the superheated section is neglected in length, meaning total evaporator pressure drop ΔP_e equals to two-phase section pressure drop ΔP_{tpe}.

$$\Delta P_e = \Delta P_{tpe} \tag{31}$$

However, the condenser is divided into two main sections and the total pressure drop is the sum of the of two-phase section ΔP_{tpc} and vapor section ΔP_{vc} pressure drops.

$$P_c = \Delta P_{tpc} + \Delta P_{vc} \tag{32}$$

The length of the two-phase section is determined by the proportion of heat transfer areas:

$$\frac{L_{tpc}}{L_c} = \frac{A_{c2}}{A_{c1}+A_{c2}} \tag{33}$$

The Darcy-Weisbach equation [32] is used to calculate frictional pressure drop in single-phase flow:

$$\Delta P_f = \frac{f_v L_v (v_m)}{D_h} G^2 \tag{34}$$

The Blasius correlation for smooth pipes is used to determine the Darcy friction factor for vapor flow f_v in the first section of the condenser:

$$f_v = \frac{0.184}{{Re_v}^{0.2}} \tag{35}$$

This correlation is valid for $2.10^4 < Re_v \leq 2.10^6$, which aligns well with the Reynolds number range relevant to heat pump modeling.

2.2. Solution Procedure

This study investigates how system performance and parameters change when different types of refrigerants are used in the same ASHP. A 4.6 kW heating capacity inverter-type split air conditioner was selected as the reference system. The system was modeled in MS-Excel using the technical data provided by the air conditioner manufacturer, as listed in Table 2, and the equations defined in Section 2.1.

Table 2. Technical data of reference air conditioner [33, 34]

Technical data	**FTXF42E5V1B RXF42E5V1B**
Refrigerant type	R32
COP at 7°C Tout (0,9 RH), 20°C Tin, at 4600W heat load	3.71
Evaporator air flow rate and power	27.5 m^3/min – 30 W
Condenser air flow rate and power	12.8 m^3/min – 50 W
Global efficiency of compressor	0.7
Isentropic efficiency of compressor	0.85
Evaporator's NTU	2
Evaporator pipe length (m)	31
Condenser pipe length (m)	22
Evaporator pipe inside diameter (mm)	10
Condenser pipe inside diameter (mm)	7

The solution steps for modeling the reference system are detailed in Fig. 4. The CoolProp plugin was used to determine the thermodynamic properties of the refrigerant, while the Solver plugin facilitated the iterative adjustment of variables to satisfy desired equations in MS-Excel.

The reference system model using R32 refrigerant was developed, and the evaporator and condenser logarithmic mean temperature differences ($\Delta T_{me}|_{r1}, \Delta T_{mc2}|_{r1}$) were determined by solving the system. When remodeling the system for different refrigerants, changes in these values were recalculated based on variations in temperature and heat load. The solution was achieved by ensuring equality between both methods.

The system was first solved by neglecting pressure drops in the evaporator and condenser. After obtaining the initial solution, the calculated evaporator pressure drop (ΔP_{re}) was subtracted from the evaporator pressure (P_{re}) to determine the evaporator outlet pressure (P_{reo}), while the evaporator inlet pressure (P_{rei}) was kept equal to P_{re}. Similarly, the condenser pressure drop (ΔP_{rc}) was added to the condenser pressure (P_{rc}) to determine the condenser inlet pressure (P_{rci}), while the condenser outlet pressure (P_{rco}) was kept equal to P_{rc}. The system was then solved again with these updated pressure values:

$$P_{reo} = P_{rei} - \Delta P_{re} \tag{36}$$

$$P_{rci} = P_{rco} + \Delta P_{rc} \tag{37}$$

The same procedure was repeated for varying outdoor air conditions (0°C and 15°C), and the performances of the refrigerants under different conditions were evaluated. The solution process for refrigerant and outdoor temperature changes is detailed in Fig. 5.

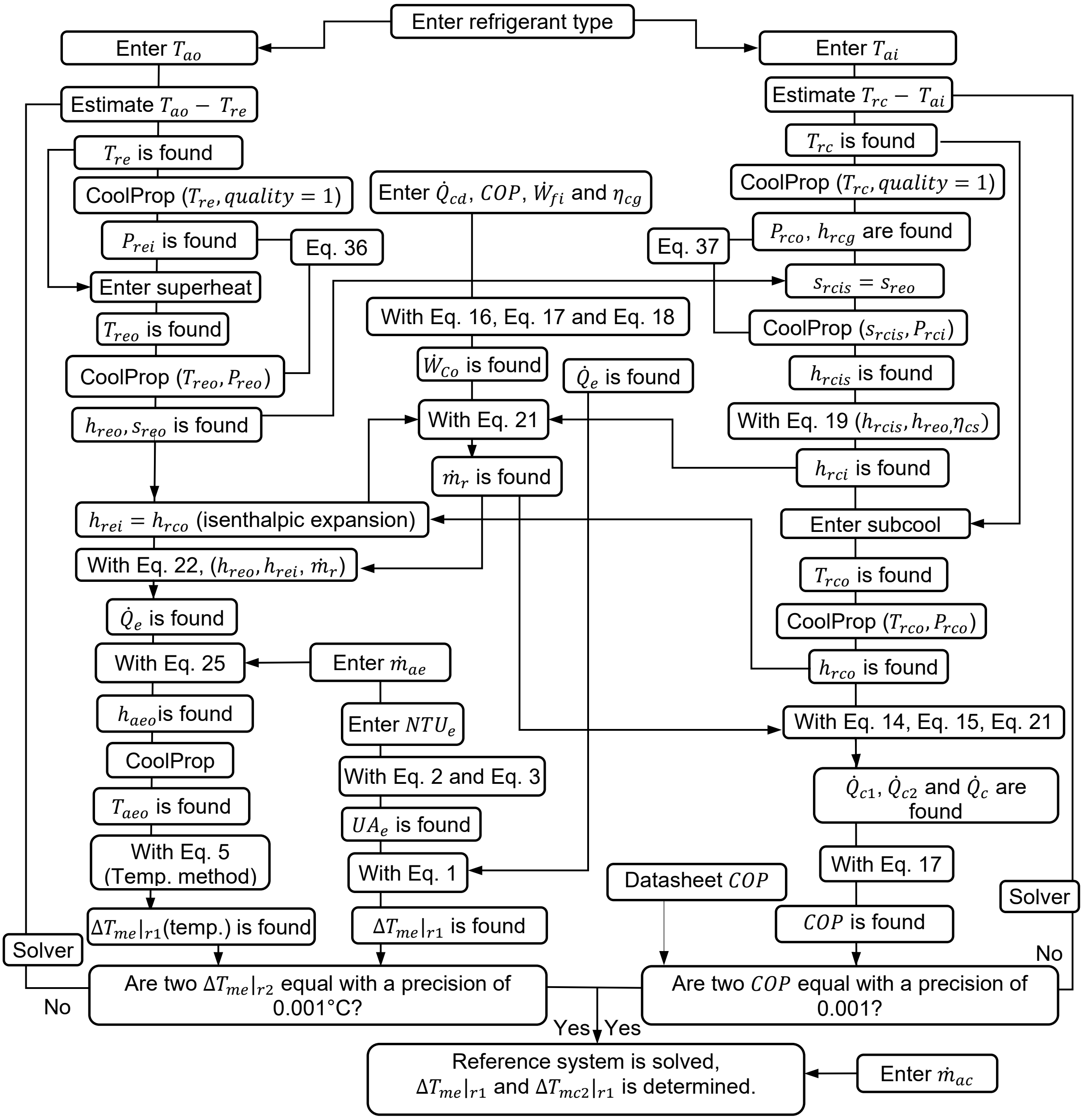

Figure 4. The solution steps for modeling the reference system

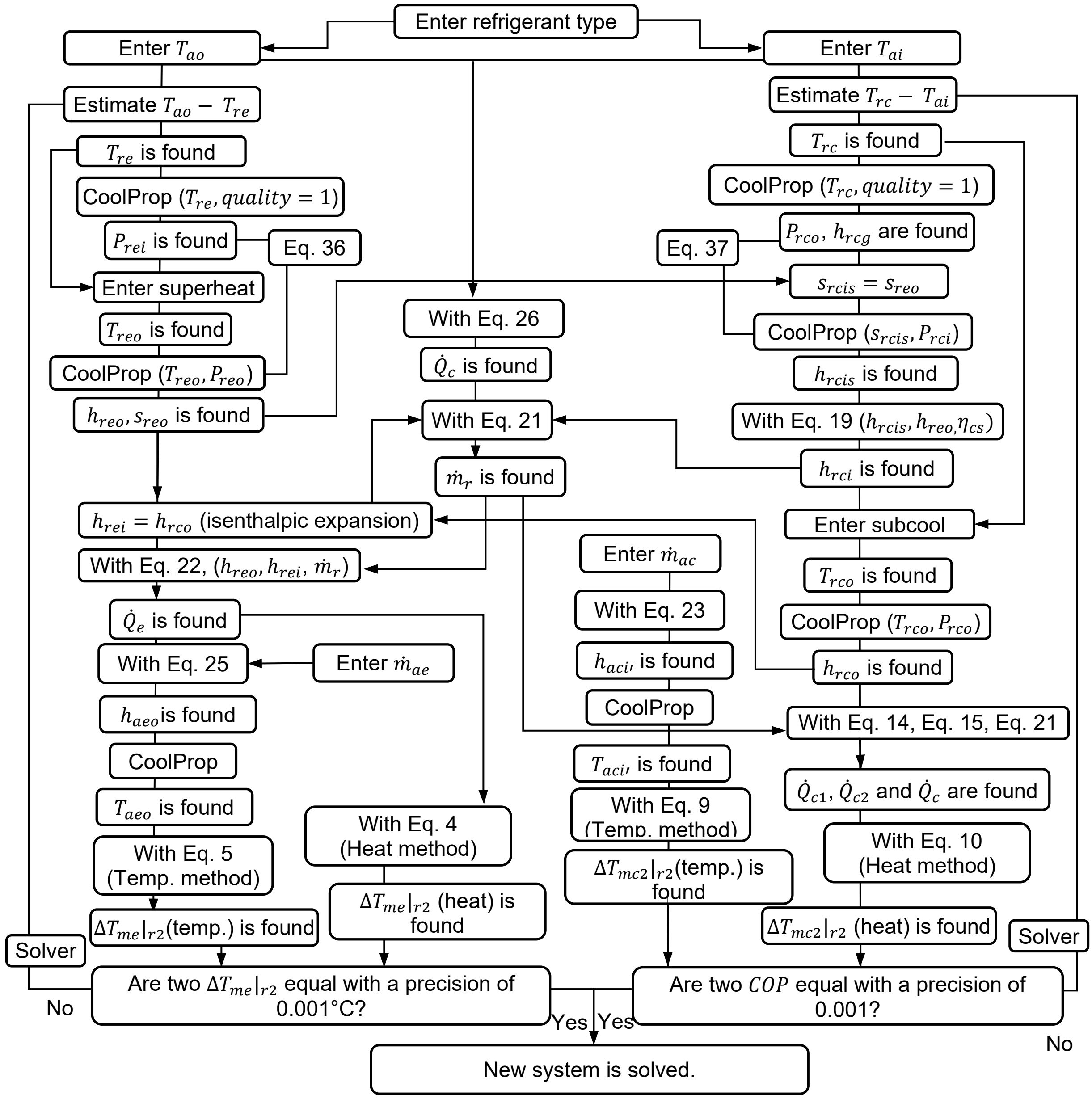

Figure 5. Solution steps for the model considering refrigerant and outdoor temperature changes

2.3. Model Validation

The validation of the model was conducted using performance test data provided by the manufacturer for three air conditioners utilizing R22, R410A, and R32 refrigerants under varying outdoor temperature conditions. Unfortunately, since air conditioners using R290 and R1234ze(E) refrigerants have not yet been commercialized and are unavailable in the market, manufacturer test data for these refrigerants could not be obtained. As a result, model predictions for these refrigerants could not be experimentally validated.

In Table 3, the model's COP predictions are compared with the manufacturer's experimental data for the three air conditioning systems using R22, R410A, and R32 refrigerants. The coefficient of determination (R2) values of air conditioners using R22, R410A, and R32 are 0.889, 0.918, and 0.912, respectively. These results indicate a reasonable level of agreement between the model predictions and the experimental data, demonstrating the model's capability to accurately simulate the performance of the air conditioning systems under the tested conditions.

Table 3. Comparison of model results with manufacturers test data

Air Conditioner Model	**T_{out} (T_{in}: 20°C)**	**COP_{exp}**	**COP_{model}**	**R2**
WMZ12-	15°C	2.95	2,92	
GCZ12 [35]	10°C	2.86	2,83	0.889
Refr. : R22	7°C	2.77	2,77	
FTXB35C2V1B-	10°C	3.92	3.81	
RXB35C2V1B [36]	7°C	3.72	3.72	0.918
Refr. : R410A	0°C	3.38	3.39	
FTXF42E5V1B	10°C	2.91	3.09	
RXF42E5V1B [33]	-5°C	3.26	3.30	0.912
Refr. : R32	-10°C	3.92	3.81	

To address the lack of experimental data for R290 and R1234ze(E), pressure (P) - specific enthalpy (h) diagrams were generated for all five refrigerants (R22, R410A, R32, R290, and R1234ze(E)) under the reference conditions using the developed model. These diagrams, shown in Figure X, provide a visual comparison of the thermodynamic cycles and further validate the model's accuracy for all refrigerants. The cycles for R290 and R1234ze(E) exhibit the expected behavior, confirming that the model reliably predicts their performance despite the absence of experimental data.

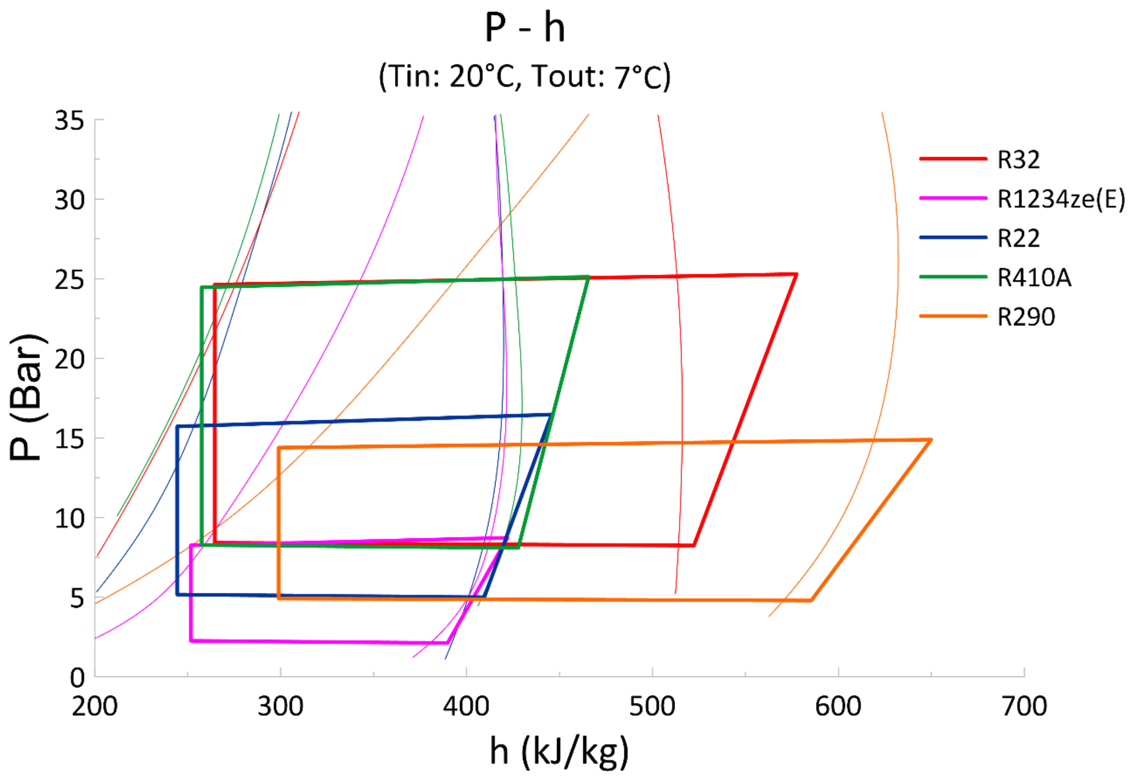

Figure 6. Pressure (P) - specific enthalpy (h) diagrams for R22, R410A, R32, R290, and R1234ze(E) under reference conditions

While pressure drops in the evaporator and condenser are included in the theoretical model, their magnitudes remain relatively small under the evaluated operating conditions. For example, at an outdoor temperature of 7 °C, the evaporator and condenser pressure drops are calculated as 16 kPa and 70 kPa for R22, 18 kPa and 55 kPa for R32, 12 kPa and 49 kPa for R290, and 13 kPa and 44 kPa for R1234ze(E). These pressure drops were also incorporated into the P-h diagrams; however, due to their limited magnitude, the corresponding pressure variations during the phase change processes are not readily distinguishable, and the diagrams may visually resemble idealized isobaric transitions.

3. RESULTS AND DISCUSSION

The performance and operating parameter variations of an air source heat pump (ASHP) were analyzed using a developed physics-based mathematical model when five different refrigerants (R32, R410A, R22, R290, and R1234ze(E)) were employed. An inverter-type split air conditioner with a nominal heating capacity of 4.3 kW, operating with R32 refrigerant, was used as the reference system.

It was assumed that the refrigerants were retrofitted into the system for the analysis. However, this is a hypothetical assumption, as in practice, the compressor would need to be replaced for compatibility with each refrigerant type. Additionally, evaporator and condenser pipe diameters have been adjusted to prevent excessive pressure drop for each refrigerant, ensuring optimal system performance.

3.1. Performance Comparison

Each system was examined and compared under three different outdoor conditions: 0°C, 7°C, and 15°C. The outdoor relative humidity was set to 30% at 0°C to prevent icing, and to 90% at 7°C and 15°C to comply with the manufacturer's test conditions. The performance comparison of systems utilizing different refrigerant types is presented in Fig. 7.

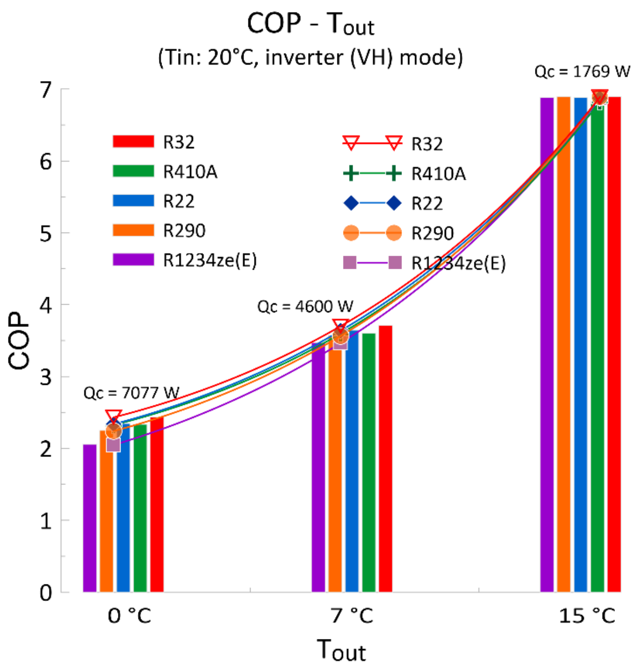

Figure 7. COP values under various outdoor air temperatures T_{out} for five different refrigerants

While the performances of the refrigerants do not show critical differences, their effectiveness can still be compared, especially under varying conditions. Among the refrigerants examined, R1234ze(E) and R290, which are considered environmentally friendly due to their low GWP values, unfortunately exhibit the poorest performance when outdoor temperatures drop to 0°C. At 0°C outdoor conditions, the R32 refrigerant achieves a COP of 2.49, whereas R1234ze(E) only reaches a COP of 2.25. Similarly, R290 performs poorly compared to R32 at lower outdoor temperatures, achieving a COP of 2.29.

R410A refrigerant demonstrates a performance trend similar to R32 at varying outdoor temperatures, but its COP values remain consistently lower across all conditions. For outdoor temperatures of 0°C, 7°C, and 15°C, the COP values for R32 and R410A are 2.49–2.35, 3.71–3.59, and 6.84–6.77, respectively.

The R22 refrigerant, though no longer used in new systems but still present in older air conditioners, exhibits slightly better performance than R32 at outdoor temperatures of 7°C and 15°C, but worse performance at 0°C. The COP values for R22 at 0°C, 7°C, and 15°C are 2.45, 3.71, and 6.90, respectively.

3.2. Advantages and Disadvantages of Each Refrigerant in Terms of CO2 Equivalence

In the context of the Kigali Amendment, which aims to phase down high-GWP refrigerants, the environmental impact of each refrigerant is a critical consideration. R22, with an ODP of 0.055 and a GWP of 1810, is being phased out globally due to its ozone-depleting potential and high climate impact. R410A, while having zero ODP, has a high GWP of 2088, making it a target for replacement under the Kigali Amendment. R32, with a GWP of 677, represents a significant improvement over R410A, but its mild flammability (A2L classification) requires careful handling. R290 (propane) and R1234ze(E) are the most environmentally friendly options, with GWPs of 3.0 and 6.0, respectively. However, R290's high flammability (A3 classification) and R1234ze(E)'s high cost and lower performance at low temperatures present challenges for widespread adoption.

3.3. Refrigerant Charge Ranges and System Design Implications

Although the total amount of refrigerant required by the system was not calculated in this study, the refrigerant mass flow rates circulating in the system were determined, along with their variations based on external temperature, as shown in Table 4. An increase in the mass flow rate would necessitate larger pipe diameters in the evaporator and condenser to prevent pressure losses, as well as an increase in compressor volume. Consequently, the refrigerant charge in the system would also increase. Table 5 presents data from studies comparing refrigerant charges. While specific conditions—such as heating or cooling load and ambient conditions—were not examined, the refrigerant flow rate data obtained in this study can serve as a general indication of refrigerant charge requirements.

Table 4. Refrigerants flow rates at various outdoor conditions

Refrigerant	Tout : 0°C	Tout : 7°C	Tout : 15°C
R22	35.49 g/s	23.30 g/s	8.95 g/s
R410A	34.62 g/s	22.53 g/s	8.53 g/s
R32	22.06 g/s	14.92 g/s	5.87 g/s
R290	21.36 g/s	13.37 g/s	4.93 g/s
R1234ze(E)	45.47 g/s	27.79 g/s	10.04 g/s

Table 5. Comparison of refrigerant charge amounts from other studies

Compared refrigerant charges	Result
R32 vs R22 at cooling [37]	R32 charge amount is 82% of R22
R290 vs R22 at cooling [38]	R290 needs 40-55% less charge than R22
R290 vs R410A at cooling [16]	R290 charge amount is 45-55% of R410A
R1234ze(E) at 1.6kW vs R410A at 2.8kW heating [39]	At same heating capacity R1234ze(E) is expected 10% higher charge.

Among the analyzed refrigerants, R290 exhibits the lowest mass flow rate requirements, followed closely by R32. In contrast, R1234ze(E) has the highest refrigerant flow rate under all three conditions. Under high heating load at 0°C, R1234ze(E) has a flow rate 2.06 times higher than R32, decreasing to 1.71 times higher at 15°C. R410A and R22 have similar refrigerant flow rates, which are approximately 65% higher than R32 across all three conditions.

A similar proportional correlation between refrigerant charges is observed in the studies compiled in Table 4. In the study by Koyama et al., R1234ze(E) exhibited flow rates close to those of R410A for nearly half the heating load, indicating that the flow rate of R1234ze(E) would increase under equal heating loads.

The pipe diameter values where the evaporator and condenser pressure drops are minimized have been determined for each refrigerant. The pressure drops are shown in Table 6. Unfortunately, since R410A is a mixed refrigerant, the pressure drop could not be calculated directly. Therefore, the pressure drop values of R32 have been applied to R410A as an approximation. The pipe diameter values, optimized to minimize performance loss, reveal that R1234ze(E) requires larger pipe diameters to mitigate high pressure losses, which will increase system costs. Additionally, larger pipe diameters will increase the refrigerant charge amount, further impacting system design and operational costs. In contrast, R290, despite being a next-generation refrigerant, requires smaller pipe diameters compared to R1234ze(E). R32 exhibits the least pressure loss and can be used with the smallest pipe diameters, making it a cost-effective and efficient choice for system design.

Table 6. Pressure drop and pipe diameter requirements for each refrigerant

Refrigerant			Pressure Drop (kPa)					
			Tout : 0°C		Tout : 7°C		Tout : 15°C	
	Evap. Tube (OD) Ø (mm)	Cond. Tube (ID) Ø (mm)	Evap.	Cond.	Evap.	Cond.	Evap.	Cond.
R22	12	8	47	108	16	70	2	19
R32	10	7	49	87	18	55	2	14
R290	12	8	36	77	12	49	1	12
R1234ze(E)	15	10	40	62	13	44	2	12

OD: Outdoor unit , ID: Indoor unit, Ø: diameter

3.4. Condenser and Evaporator Pressures

The condenser pressure values, representing the high-pressure zone of the air conditioner, are presented in Fig. 8. Based on these values, R32 and R410A can be categorized as high-condensing-pressure refrigerants, R22 and R290 as medium-condensing-pressure refrigerants, and R1234ze(E) as a low-condensing-pressure refrigerant. Under outdoor conditions of 7°C, the condenser pressure values for R32, R410A, R22, R290, and R1234ze(E) are calculated as 25.6, 25.4, 16.4, 14.9, and 8.6 bar, respectively.

The low condensing pressure of the environmentally friendly and innovative R1234ze(E) refrigerant offers several advantages, including safer and more economical manufacturing of condensers and piping, as well as enhanced protection against potential system leaks, despite its high price. Similarly, the fact that R290 has 60% lower condenser pressure compared to R32 ensures that the sealing of this highly flammable yet environmentally friendly gas can be achieved more safely.

The evaporator pressure also varies similarly to the condenser pressure depending on the refrigerant type, as illustrated in Fig. 9. Under outdoor conditions of 7°C, the evaporator pressure values for R32, R410A, R22, R290, and R1234ze(E) were calculated as 8.4, 8.3, 5.2, 4.9, and 1.5 bar, respectively.

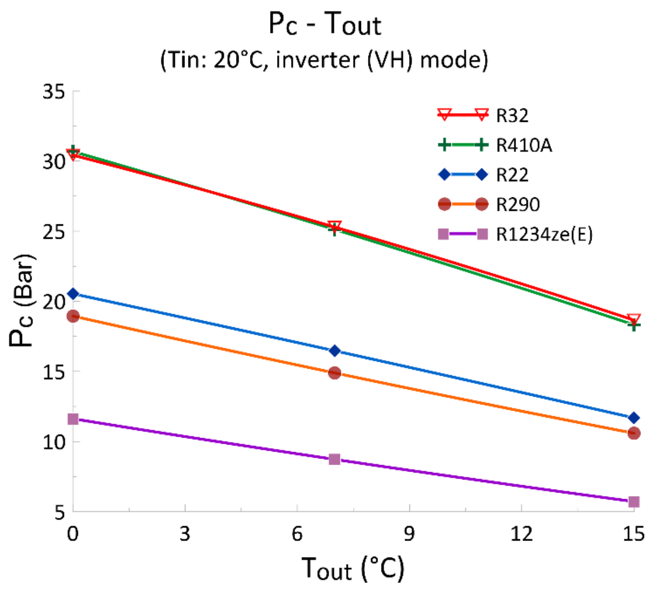

Figure 8. The condenser pressure P_c under various outdoor air temperatures T_{out} for five different refrigerants

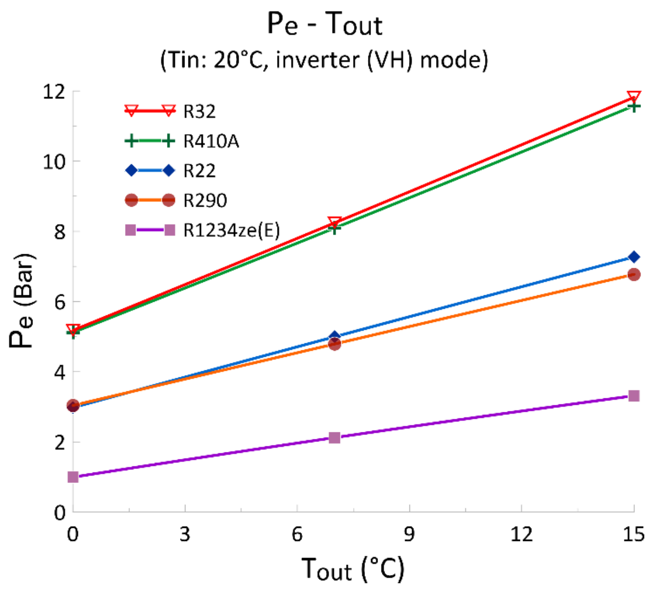

Figure 9. The evaporator pressure P_e under various outdoor air temperatures T_{out} for five different refrigerants

3.5. Condenser and Evaporator Temperatures

The condenser temperature, defined as the condensation temperature of the refrigerant in the condenser, shows similar values for the five refrigerants at higher outdoor temperatures but begins to diverge as the outdoor temperature decreases, as shown in Fig. 10. At 0°C outdoor temperature, the condenser temperature rankings from highest to lowest are R1234ze(E), R290, R22, R410A, and R32, with corresponding values of 57.2°C, 55.8°C, 53.0°C, 51.3°C, and 49.8°C. Notably, R1234ze(E) condenses at a temperature 7.4°C higher than R32 under 0°C outdoor conditions in ASHPs condenser. This temperature difference narrows to 3.2°C at 7°C outdoor temperature and further decreases to 0.5°C at 15°C outdoor temperature.

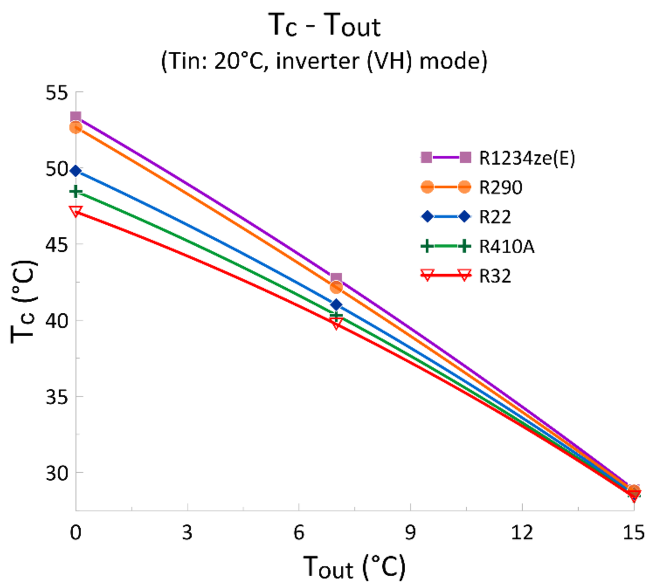

Figure 10. The condenser temperature T_c under various outdoor air temperatures T_{out} for five different refrigerants

The evaporator temperatures of the examined refrigerants are nearly identical as shown in Fig. 11, with only minor differences (up to 0.5°C) becoming noticeable at an outdoor temperature of 0°C. At this condition, R32, the refrigerant with the lowest evaporator temperature, has a value of -10.7°C, while R1234ze(E), the refrigerant with the highest evaporator temperature, reaches -10.2°C.

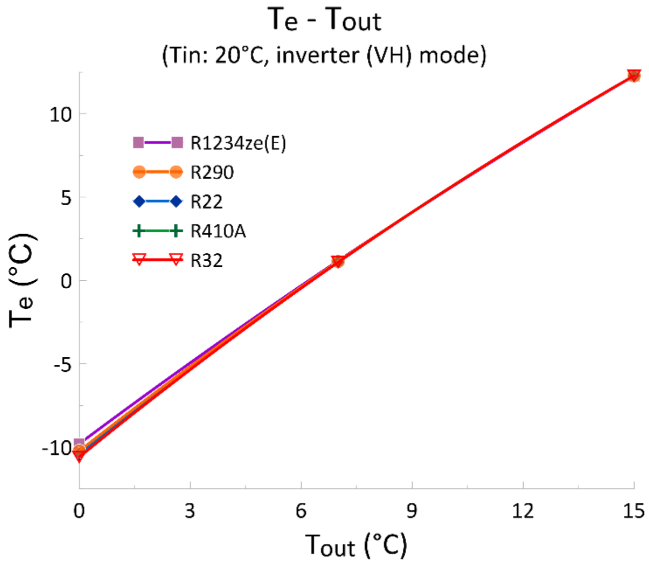

Figure 11. The evaporator temperature T_e under various outdoor air temperatures T_{out} for five different refrigerants

Additionally, the temperature–specific entropy (T–s) diagrams of the refrigerants under reference conditions (7 °C outdoor and 20 °C indoor air temperatures) are presented in Fig. 12. The evaporation temperatures of all five refrigerants are nearly identical, while their condensation temperatures exhibit relatively small variations. However, notable differences are observed in the compressor outlet (condenser inlet) temperatures. R32 has the highest compressor outlet temperature at 84.7 °C, while R1234ze(E) shows the lowest at 53.7 °C. This lower temperature may allow the use of sealing or electrical insulation materials rated for less demanding thermal conditions. R290 also exhibits a relatively low compressor outlet temperature (58.1 °C), which is advantageous in enhancing system safety for this flammable refrigerant.

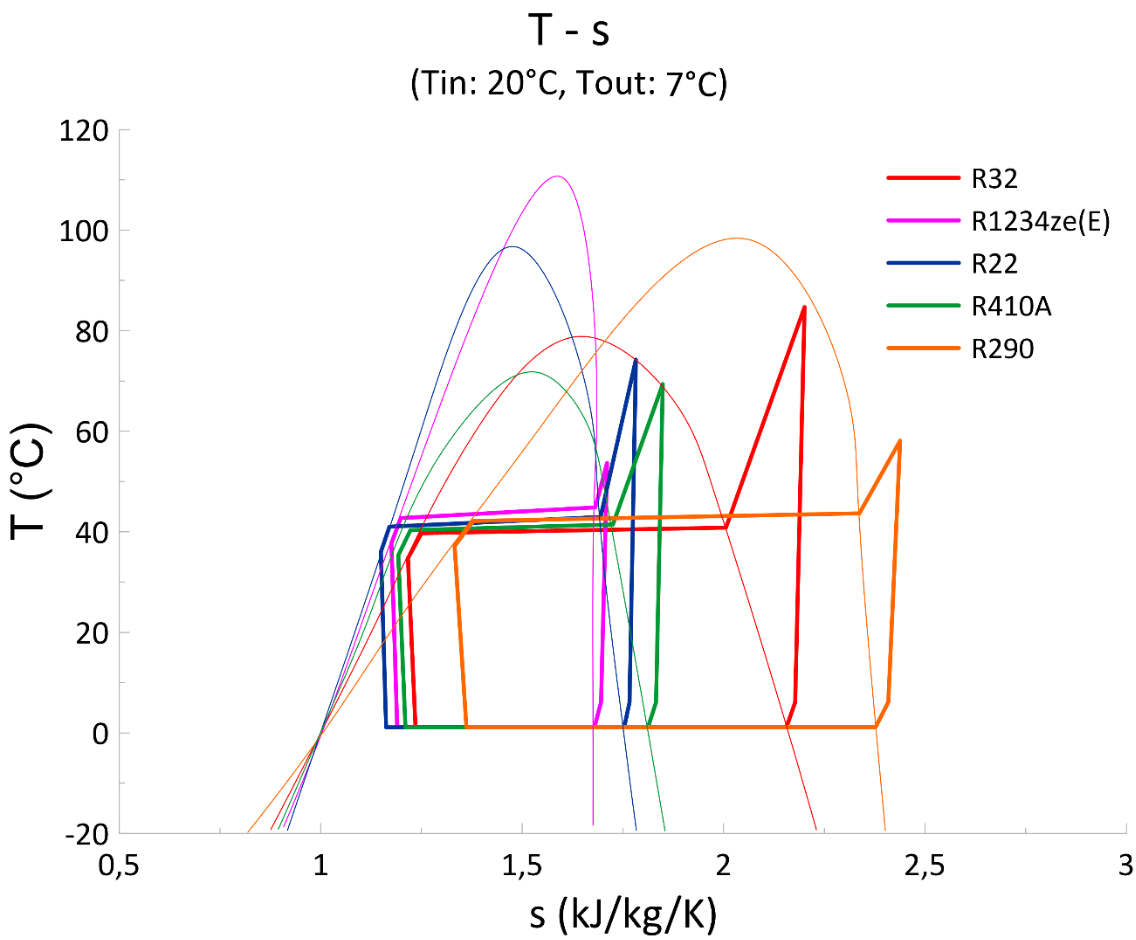

Figure 12. Temperature–specific entropy (T–s) diagrams for R22, R410A, R32, R290, and R1234ze(E) under reference conditions

3.6. Summary

Based on the findings, R32 emerges as the most advantageous alternative refrigerant for ASHPs in the near term. It offers a balance between performance, environmental impact, and system design requirements. However, with the potential for more stringent environmental regulations in the future, R32 may eventually be phased out due to its moderate GWP (677). This highlights the need for continued research and development of ultra-low-GWP alternatives.

Among the next-generation refrigerants, R290 (propane) and R1234ze(E) are promising candidates. R290 has the lowest GWP (3.0) and requires the smallest refrigerant charge, making it highly environmentally friendly. However, its high flammability (A3 classification) poses significant safety challenges, limiting its widespread adoption. On the other hand, R1234ze(E) has an ultra-low GWP (6.0) and low flammability (A2L classification), but its higher cost, lower performance at low temperatures, and larger pipe diameter requirements make it less favorable for immediate use.

In the long term, R290 may be the preferred choice for applications where safety concerns can be effectively managed, while R1234ze(E) could become more viable as technological advancements reduce its costs and improve its performance. Both refrigerants represent critical steps toward achieving sustainable and environmentally friendly ASHP systems, but further innovation is needed to address their respective limitations.

4. CONCLUSSIONS

In this study, the changes in ASHP performance and operating parameters were analyzed when five different refrigerants were retrofitted into the same air source heat pump (ASHP), utilizing a developed physics-based model. R22 and R410A were considered as phased-out refrigerants due to their ozone depletion and greenhouse gas effects, while R32, R290, and R1234ze(E) were evaluated as pure gas alternatives developed in response to these environmental concerns. Each refrigerant was assessed under three different outdoor temperature conditions (0°C, 7°C, and 15°C), and their effects were compared based on the varying operational parameters.

Although no critical difference is observed between the performances of the refrigerants, a comparison can still be made, particularly under varying conditions. R32 offers a higher COP, especially at low outdoor temperatures. In contrast, R1234ze(E), the most environmentally friendly option due to its low GWP, shows lower performance in cold conditions but improves significantly as temperatures rise, outperforming others at 15°C. R290, a next-generation refrigerant, demonstrates performance between R32 and R1234ze(E) across all conditions. R32, which dominates today's market, performs strongly in moderate and cold conditions, but its use will be restricted in the future as stricter environmental regulations come into effect.

Refrigerant flow rates offer insights into the refrigerant charge requirements. R1234ze(E) has the highest flow rate, nearly twice that of R290 and R32. Given the high cost of R1234ze(E), this is expected to significantly impact charging costs. However, the low condenser and evaporator pressure provided by R1234ze(E) allows the use of lower cost equipment. R410A and R22, which are being phased out, require higher flow rates and refrigerant charges compared to R32 and R290.

Pressure drop and pipe diameter requirements also play a critical role in system design. R1234ze(E) requires larger pipe diameters to mitigate high pressure losses, which increases system costs and refrigerant charge amounts. In contrast, R32 exhibits the least pressure loss and can be used with smaller pipe diameters, making it a cost-effective choice. R290, despite requiring slightly larger pipes than R32, operates at lower condenser and evaporator pressures, enhancing system safety and reducing sealing challenges. This characteristic, combined with its low GWP, makes R290 a promising next-generation refrigerant, although its high flammability remains a significant concern.

Condenser and evaporator temperature trends were largely similar across refrigerants, with R32 consistently showing the lowest condensing temperature under low outdoor temperature conditions.

In summary, R32 is the most advantageous refrigerant for current ASHP systems, balancing performance, environmental impact, and design requirements. R290 and R1234ze(E) represent promising next-generation alternatives, with R290 offering the lowest GWP and charge requirements, and R1234ze(E) providing ultra-low GWP and low flammability. However, R290's high flammability and R1234ze(E)'s higher cost and lower performance at low temperatures present challenges. Both refrigerants are critical for achieving sustainable ASHP systems in the future.

The comparative analyses in this study provide valuable insights for researchers seeking environmentally friendly, safe, and efficient refrigerants. Future studies could include precise calculations of refrigerant charge requirements and cost analyses for various climate zones.

NOMENCLATURE

Symbols		Subscripts	
A	heat transfer surface area (m^2)	a	air
C	heat capacity (W/K)	acc	acceleration
c	specific heat (J/kg.K)	$c1$	condensers first region
D_h	hydraulic diameter (m)	$c2$	condensers second region
f_N	two-phase friction factor	e	evaporator
g	gravitational acceleration (m/s^2)	f	fan
G	Mass flux (kg/m^2s)	fr	friction
h	enthalpy (J/kg)	i	in
K_f	two-phase number	n	new condition
L	length (m)	o	out
$\dot{m}$	mass flow rate (kg/s)	r	refrigerant
NTU	number of transfer units	s	isentropic
P	pressure (Pa)	tp	two-phase
Re_{fo}	liquid only Reynolds number	v	vapor
$\dot{Q}$	heat load (W)	0	reference condition
T	temperature (K)	Abbreviations	
U	heat transfer coefficient ($W/m^2.K$)	ASHP	Air source heat pump
v	specific volume (m^3/kg)	COP	Coefficient of performance
$\dot{W}$	power (W)	GWP	Global warming potential
x	vapor quality	HC	Hydrocarbon
η_{cs}	compressor isentropic efficiency	HFC	Hydrofluorocarbon
η_{cg}	compressor global efficiency	HCFC	Hydrochlorofluorocarbon
ΔT_m	logarithmic mean temp. diff. (K)	HFO	Hydrofluoroolefin
ΔP	pressure drop (Pa)	ODP	Ozone depletion potential
μ_f	dynamic viscosity – liquid only (Pa s)	VH	variable heat (inverter) mode

DECLARATION OF ETHICAL STANDARDS

The author of the paper submitted declares that nothing which is necessary for achieving the paper requires ethical committee and/or legal-special permissions.

CONTRIBUTION OF THE AUTHORS

Kutbay Sezen: Conceptualization, Analysis; Writing- review & editing.

CONFLICT OF INTEREST

There is no conflict of interest in this study.

REFERENCES

[1] Yang Z, Wu X. Retrofits and options for the alternatives to HCFC-22. Energy 2013; 59: 1-21.

[2] Zhang Y, Yang Z, Chen Y, He H, Zhao Y. Life cycle climate performance of R410A and its environmentally friendly alternative working fluids in a heat pump system. Sustainable Energy Technologies and Assessments 2024; 71: 104020.

[3] Heath EA. Amendment to the Montreal protocol on substances that deplete the ozone layer (Kigali amendment). International Legal Materials 2017; 56(1): 193-205.

[4] Böhringer C. The Kyoto protocol: a review and perspectives. Oxford Review of Economic Policy 2003; 19(3): 451-66.

[5] Mota-Babiloni A, Navarro-Esbrí J, Makhnatch P, Molés F. Refrigerant R32 as lower GWP working fluid in residential air conditioning systems in Europe and the USA. Renewable and Sustainable Energy Reviews 2017; 80: 1031-42.

[6] Astina IM, Alfisahri HI. New thermodynamic equation of state for refrigerant HFO-1243zf. International Journal of Thermodynamics 2023; 26(4): 19-30.

[7] Tamene Y, McHounchi L, Madanı H, Mehemmai M. Performances study of eco-friendly binary azeotropic mixtures used as working fluid in three refrigeration cycles. International Journal of Thermodynamics 2024; 27(4): 1-13.

[8] Yadav S, Liu J, Kim SC. A comprehensive study on 21st-century refrigerants - R290 and R1234yf: a review. International Journal of Heat and Mass Transfer 2022; 182: 121947.

[9] Arpagaus C, Bless F, Uhlmann M, Schiffmann J, Bertsch SS. High temperature heat pumps: market overview, state of the art, research status, refrigerants, and application potentials. Energy 2018; 152: 985-1010.

[10] Choudhari C. Experimental study of hydrocarbon r290 in water cooler refrigeration system. Journal of Thermal Engineering 2020; 6(1): 43-9.

[11] Polonara F, Kuijpers L, Peixoto R. Potential impacts of the Montreal protocol Kigali amendment to the choice of refrigerant alternatives. International Journal of Heat Technology 2017; 35(1): 1-8.

[12] Lemmon EW, Bell IH, Huber M, McLinden M. NIST standard reference database 23: reference fluid thermodynamic and transport properties. National Institute of Standards and Technology, Gaithersburg, US, 2018.

[13] Shaik SV, Babu TPA. Theoretical computation of performance of sustainable energy efficient R22 alternatives for residential air conditioners. Energy Procedia 2017; 138: 710-716.
[14] Martins LVS, Braga CHM, Pabon JJG, Machado L, Duarte WM. Assessment of total equivalent warming impact (TEWI) of alternative refrigerants for retrofit of R22 in single split air conditioning system. Journal of Building Engineering 2024; 88: 109085.
[15] Katircioğlu F, Cingiz Z, Çay Y, Gürel AE, Kolip A. Performance assessment of a refrigeration system charged with different refrigerants using infrared image processing techniques. Arabian Journal for Science and Engineering 2021; 46(12): 12009-28.
[16] Berkah Fajar TK, Restu Bagas P, Ukhi S, Alhamid MI, Lubis A. Energy and exergy analysis of an R410A small vapor compression system retrofitted with R290. Case Studies in Thermal Engineering 2020; 21: 100671.
[17] Guilherme ÍF, Marcucci Pico DF, dos Santos DDO, Bandarra Filho EP. A review on the performance and environmental assessment of R-410A alternative refrigerants. Journal of Building Engineering 2022; 47: 103847.
[18] Tian Q, Cai D, Ren L, Tang W, Xie Y, He G, et al. An experimental investigation of refrigerant mixture R32/R290 as drop-in replacement for HFC410A in household air conditioners. International Journal of Refrigeration 2015; 57: 216-28.
[19] Mota-Babiloni A, Mateu-Royo C, Navarro-Esbrí J, Barragán-Cervera Á. Experimental comparison of HFO-1234ze(E) and R-515B to replace HFC-134a in heat pump water heaters and moderately high temperature heat pumps. Applied Thermal Engineering 2021; 196: 117256.
[20] Zhang X, Li Y. A review of recent research on hydrofluoroolefin (HFO) and hydrochlorofluoroolefin (HCFO) refrigerants. Energy 2024; 311: 133423.
[21] Salhi K, Mohamed Ramadan K, Hadjiat MM, Hamidat A. Energetic and exergetic performance of solar-assisted direct expansion air-conditioning system with low-GWP refrigerants in different climate locations. Arabian Journal for Science and Engineering 2020; 45(7): 5385-98.
[22] Ibrahim OAA, Kadhim SA, Hammoodi KA, Rashid FL, Askar AH. Review of hydrocarbon refrigerants as drop-in alternatives to high-GWP refrigerants in VCR systems: The case of R290. Cleaner Engineering and Technology 2024; 23: 100825.
[23] Choudhari CS, Sapali SN. Performance investigation of natural refrigerant R290 as a substitute to R22 in refrigeration systems. Energy Procedia 2017; 109: 346-52.
[24] Aisyah N, Ariyadi HM. Performance evaluation of R1224yd as alternative to R123 and R245fa for vapor compression heat pump system. International Journal of Thermodynamics 2024; 27(1): 13-21.

[25] Koşan M. Investigation of using low GWP alternatives to replace R404A in the refrigeration system. International Journal of Energy Studies 2023; 8(3): 453-64.

[26] Stegou-sagia A, Damanakis M. Thermodynamic correlations, k – exponents, speed of sound, and COP data for binary refrigerant mixtures. International Journal of Thermodynamics 2004; 7(1): 15-22.

[27] Ravi G, Adhimoulame K. Thermodynamics studies on VCRS using refrigerant blends of R290, R600A, and R1234ZE. Multiscale and Multidisciplinary Modeling, Experiments and Design 2024; 7(5): 4807-18.

[28] Sezen K, Gungor A. Performance analysis of air source heat pump according to outside temperature and relative humidity with mathematical modeling. Energy Conversion and Management 2022; 263: 115702.

[29] Sezen K. Influence of airflow rates on air source heat pump operating parameters. Applied Thermal Engineering 2023; 233: 121123.

[30] Bell IH, Wronski J, Quoilin S, Lemort V. Pure and pseudo-pure fluid thermophysical property evaluation and the open-source thermophysical property library coolprop. Industrial and Engineering Chemistry Research 2014; 53(6): 2498-508.

[31] Choi YJ, Kedzierski MA, Domanski PA. A generalized pressure drop correlation for evaporation and condensation of alternative refrigerants in smooth and micro-fin tubes. National Institute of Standards and Technology, Gaithersburg, US, 1999. https://nvlpubs.nist.gov/nistpubs/Legacy/IR/nistir6333. pdf.

[32] Koopman T, Zhu T, Rohlfs W. Performance evaluation of air-source heat pump based on a pressure drop embedded model. Heliyon 2024; 10:4

[33] Daikin. RXF-E outdoor units datasheet. Daikin Industries, 2023. https://e2e.si/wp-content/uploads/2023/04/RXF-E_Data-books_EEDEN23_English.pdf.

[34] Daikin. FTXF-E indoor units datasheet. Daikin Industries, 2023. https://e2e.si/wp-content/uploads/2023/04/FTXF-E_Data-books_EEDEN23_English.pdf.

[35] Electra. WMZ series service manual. Electra Consumer Products, 2004. http://lh.airwell-res.com/sites/default/files/imported/Electra/c18/p53/WMZ%20R407C-R22-.pdf.

[36] Daikin. RXB-C Outdoor units datasheet. Daikin Industries, 2015. https://daikin.kh.ua/wp-content/uploads/2015/06/EEDEN15-100_RXB-C.pdf.

[37] Pramudantoro TP, Sukamto E, Sumeru K, Margana AS, Sukri MF. Effect of refrigerant charge variation of R32 as drop-in replacement for R22 in air conditioning system. AIP Conference Maharashtra, India, 2018.

[38] Saravanan AL, Murugan RS, Lal DM. Investigations on charge reduction strategies to use R290 as an alternative to R22 in a split air conditioner. Experimental Heat Transfer 2017; 30(2): 126-38.
[39] Koyama S, Takata N, Fukuda S. Drop-in experiments on heat pump cycle using HFO-1234ze (E) and its mixtures with HFC-32. International Refrigeration and Air Conditioning Conference Purdue, US, 2010.